A Study of Tensile Modulus and Molecular Orientation in Drawn and Shrunk Poly(ethylene Terephthalate) Combining Refractive Index, Polarized Fluorescence, and X-Ray Diffraction Measurements

D. I. BOWER, K. K. P. KORYBUT-DASZKIEWICZ, and I. M. WARD,
Department of Physics, University of Leeds, Leeds LS2 9JT, England

Synopsis

Earlier studies of the orientation of the crystalline and amorphous regions in drawn and shrunk PET tapes by refractive index, X-ray, and polarized fluorescence measurements have been extended to include a study of Young's modulus of such samples. The results show that for samples of low crystallinity, whether drawn or drawn and shrunk, the modulus correlates well with the overall orientation, as indicated by the birefringence. For such samples the overall orientation and modulus fall with increasing shrinkage. For samples which crystallize substantially, either on drawing or subsequent shrinkage, the behavior is more complicated. In particular, for samples originally drawn at 80°C to $\lambda = 3.44$ there is a range of shrinkage temperatures for which greater shrinkage can be accompanied by a smaller loss of overall orientation and modulus because of an increase in crystallinity for the same degree of crystalline and amorphous orientation. The modulus results are discussed in the light of current understanding of the structure of oriented PET. In the case of the samples which crystallize substantially on shrinkage it is shown that changes in modulus primarily related to changes in crystallinity.

INTRODUCTION

In previous publications,[1-3] we have shown how the measurement of the polarized fluorescence of a fluorescent compound incorporated into polyethylene terephthalate (PET) prior to melt spinning and drawing can provide valuable information about the molecular orientation. An essential feature of our studies has been the combination of fluorescence measurements with refractive index measurements, X-ray diffraction data, and the results of infrared and Raman spectroscopy. The previous work has had three major aspects. First, there is the question of the relationship between the molecular orientation averages and deformation mechanisms. For the hot-drawn samples which we have studied in this series of experiments, it has been shown that the development of molecular orientation with draw ratio can be very well described by a rubber-network model, even for large draw ratios.[3] Secondly, we have been concerned with the observation that the fluorescent molecules in drawn samples of PET appear to be more highly oriented than the polymer chains. Two possible explanations of this observation have been considered, and it has been shown that the more successful explanation is that the fluorescent molecules align themselves preferentially parallel to those segments of the polymer chain in which the glycol residues are in the trans conformation.[3] Finally, we have undertaken a study of drawn and subsequently shrunk PET. The results of this study suggested that the

Journal of Applied Polymer Science, Vol. 28, 1195–1206 (1983)
 CCC 0021-8995/83/031195-12$02.20

shrinkage of PET is primarily associated with disorientation of the amorphous regions and that crystallization occurs at a later stage in the shrinkage process rather than being the predominant mechanism of shrinkage per se.[2]

In the present paper, which is concerned with uniaxially oriented samples (as were Refs. 1–3), we describe a study of the changes in Young's modulus of PET due to drawing and subsequent shrinkage. In all cases the changes in orientation were also monitored by refractive index and polarized fluorescence measurements, and the results are discussed in terms of previous understanding of the structure and mechanical properties of this polymer.

Orientation Averages

It has been established by previous investigations[1,2] that the samples under discussion here are transversely isotropic to a very good degree of approximation. It is therefore appropriate to define an orientation average $\langle P_2(\epsilon) \rangle$, which is the average value of $P_2(\epsilon)$, where ϵ is the cosine of the angle θ between the draw direction and a typical chain axis direction in the polymer. In the present paper we will be concerned with several averages of this type, obtained from refractive indices and from X-ray diffraction and polarized fluorescence measurements.

EXPERIMENTAL

Sample Preparation

Amorphous PET tapes of approximate cross-section 1.5×10^{-3} m by 1.0×10^{-4} m, containing 50–200 ppm by weight of the fluorescent compound 4-4′-(dibenzoxazolyl) stilbene, were prepared by melt spinning. These tapes were subsequently drawn over a cylinder (the "pin") maintained at 80°C, to a series of draw ratios. The heated pin was situated between two sets of rollers rotating at appropriately different rates.

The oriented tapes were then subsequently shrunk by either of two methods. The tapes with an initial draw ratio of 2 were shrunk to a controlled final length by passing them through a hot air oven at 80°C, which was located (in the place of the pin) between the feed and windup rollers of the drawing process. All other drawn tapes were shrunk by placing them in an air oven free from constraints, for a fixed period of time (in the range 10–60 min) at a temperature in the range 70–180°C.

Further details of these procedures for sample preparation have been given in previous publications.[1,2] Many of the samples were characterized in the previous investigations, although no mechanical measurements were undertaken, and these are identified in Tables I–III. Further samples were also prepared for the present studies, and details of these are shown in Table IV.

Refractive Index Measurements

The optical orientation averages $\langle P_2(\epsilon) \rangle_{\text{opt}}$, which relate to the chain axis orientation averaged over all chains, were determined by measuring the refractive index of the samples for light polarized with the electric vector parallel to the draw direction, n_z, and normal to this direction but parallel to the plane of the tape, n_x.

TABLE I
As-Drawn Samples

Sample no.	Sample no. in Ref. 2	Draw ratio λ	$\langle P_2(\epsilon)\rangle_{opt}$	$\langle P_2(\epsilon)\rangle_a$	Crystallinity	Modulus (GPa)
1	1a	2.0	0.17	0.18	0.01	2.9
2	2a	2.5	0.30	0.27	0.03	4.0
3		2.96	—	—	—	6.6
4	3a	3.44	0.59	0.58	0.06	10.9
5	3j	3.5	0.58	0.55	0.11	10.2
6		3.82	0.51	0.55	—	9.3
7	4a	4.2	0.72	0.74	0.06	10.0
8		4.4	0.73	0.78	—	11.4
9		4.85	0.75	0.64	—	

As shown in a previous publication

$$\frac{\Delta\alpha}{3\alpha_0}\langle P_2(\epsilon)\rangle_{opt} = \frac{\phi_z^e - \phi_x^e}{\phi_z^e + 2\phi_x^e} \tag{1}$$

where $\phi_i^e = (n_i^2 - 1)/(n_i^2 + 2)$, with $i = z, x$. $\Delta\alpha$ is the difference between the electronic polarizabilities of a polymer repeat unit parallel and perpendicular to the chain axis, and α_0 is the mean polarizability. Following a previous publication,[3] we have taken the value of $\Delta\alpha/3\alpha_0$ as 0.106.

Fluorescence Measurements

The fluorescence orientation averages $\langle P_2(\epsilon_M)\rangle$ relate to the orientation of an axis M fixed within the fluorescent molecule averaged over all the fluorescent molecules under observation. The fluorescence measurements involve the determination of the intensity and polarization of the fluorescence scattering when the sample is subjected to polarized exciting light of suitable wavelength. Full details of the apparatus and determination of the orientation averages have been given in a previous paper.[1]

A point of particular interest is the relationship between the fluorescence orientation averages and those for structural elements in the polymer. In a previous paper[3] on the drawing and shrinkage behavior it was concluded that the relationship between the distribution of orientation of fluorescent molecules and the polymer chains in the amorphous regions of semicrystalline PET is the same as that in completely amorphous PET. This conclusion was based on a comparison of results from refractive index, X-ray diffraction, and fluorescence

TABLE II
Samples Initially Drawn to λ = 2.0 and Shrunk at 80°C for 30 s to Controlled Final Length

Sample no.	Sample no. in Ref. 2	Final draw ratio λ	$\langle P_2(\epsilon)\rangle_a$	$\langle P_2(\epsilon)\rangle_a$	Modulus (GPa)
1	1a	2.00	0.17	0.18	2.9
10	1c	1.64	0.08	0.08	2.6
11	1d	1.43	0.04	0.04	1.8
12	1e	1.32	0.02	0.03	2.4
13	1f	1.05	0.00	0.01	2.1
14	1g	1.00	0.00	0.02	1.9

TABLE III
Samples Initially Drawn to $\lambda = 3.44$ and Shrunk Freely for 10 Min

Sample no.	Sample no. in Ref. 2	Shrinkage temp (°C)	Shrinkage (%)	Final draw ratio λ	Crystallinity	$\langle P_2(\epsilon)\rangle_{opt}$	$\langle P_2(\epsilon)\rangle_a$	$\langle P_2(\epsilon)\rangle_c$	Modulus (GPa)
4	3a	drawn only		3.44	0.06	0.59	0.58	0.54	10.9
15	3b	70	2.9	3.34	0.13	0.43	0.41	0.58	4.2
16	3c	80	9.6	3.11	0.18	0.39	0.37	0.66	4.0
17	3d	90	14.0	2.96	0.22	0.39	0.27	0.73	2.5
18	3e	100	14.8	2.93	0.28	0.50	0.30	0.76	4.5
19	3f	110	17.7	2.83	0.31	0.48	0.24	0.83	3.7
20	3g	120	16.6	2.87	0.36	0.53	0.20	0.73	3.9
21	3i	180	18.3	2.81	0.49	0.59	0.19	0.76	5.1

TABLE IV
Samples Shrunk from Various Draw Ratios 2.96–4.85[a]

Sample no.	Original draw ratio λ	Shrinkage time (min)	Shrinkage (%)	Final Draw ratio λ	$\langle P_2(\epsilon)\rangle_{opt}$	$\langle P_2(\epsilon)\rangle_a$	Modulus (GPa)
22	2.96	30	7	2.75	0.33	—	4.5
23	3.82	30	9	3.48	0.38	0.35	5.2
24	4.2	60	7	3.91	0.63	0.46	5.7
25	4.2	60[a]	8	3.86	0.64	0.45	5.8
26	4.4	60	9	4.00	0.65	0.51	6.7
27	4.85	60	9	4.41	0.69	0.66	—

[a] All tapes were shrunk at 80°C except tape 25, which was shrunk at 90°C.

measurements. It is therefore possible to use the unique relationship which was shown to exist between the birefringence of the sample and $\langle P_2(\epsilon_M)\rangle$ for samples of low crystallinity to obtain a value for $\langle P_2(\epsilon)\rangle_a$, the orientation average of the amorphous regions, from the measured value of $\langle P_2(\epsilon_M)\rangle$.

Modulus Measurements

The Young's modulus of the tapes was measured by a dead loading creep experiment as described in detail elsewhere.[4] The values quoted refer to a secant modulus calculated from the 10 s isochronal stress–strain curves with a maximum strain of 1%.

Crystallinity Measurements

The crystallinities of some of the samples were determined in Ref. 2 from their densities, using a method which allowed for changes in the density of the amorphous material with its degree of orientation.[2]

RESULTS AND DISCUSSION

Comparison of Orientation Averages from Refractive Index and Polarized Fluorescence Measurements

The values of $\langle P_2(\epsilon)\rangle_{opt}$ are shown in Figure 1 for all samples. It can be seen that with one exception the values for the drawn samples and for those shrunk samples originating from drawn samples with $\lambda = 2$ (where crystallization has not occurred on drawing) fall on a smooth sigmoidal curve. The values for the shrunk samples originating from samples with higher draw ratios do not appear to present any consistent pattern, and can lie either above or below the curve. $\langle P_2(\epsilon)\rangle_{opt}$ is essentially a measure of the overall orientation and qualitatively these results can be understood in terms of the arguments presented in our previous publication,[2] where it was shown that the thermal treatments causing shrinkage give rise to relaxation of the oriented amorphous regions to reduce the overall orientation, but can also give rise to increases in crystallinity and crystalline orientation which increase the overall orientation. On the other hand, the values of $\langle P_2(\epsilon)\rangle_a$ (Fig. 2) appear to provide more physical insight. Again, the values for the drawn samples and for the shrunk samples originating from

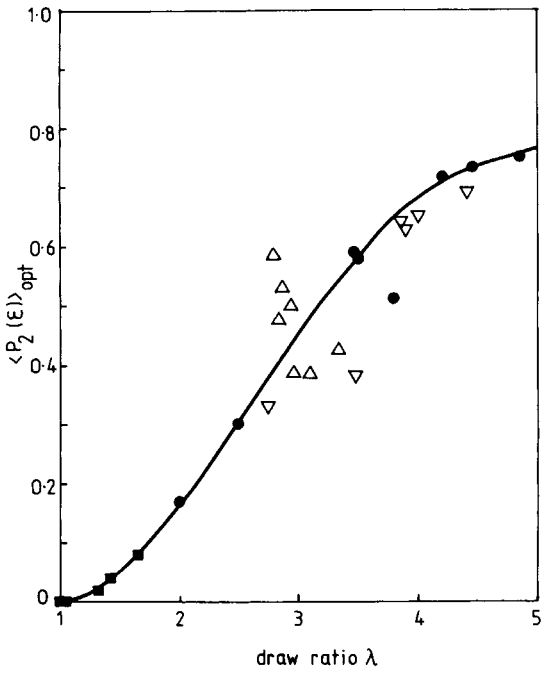

Fig. 1. $\langle P_2(\epsilon)\rangle_{opt}$ plotted against draw ratio for samples in Tables I–IV: (●) as-drawn samples (Table I); (■) shrunk from $\lambda = 2.0$ (Table II); (△) shrunk from $\lambda = 3.44$ (Table III); (▽) shrunk from various draw ratios 2.96–4.4 (Table IV). Line is smooth curve through ●, ■.

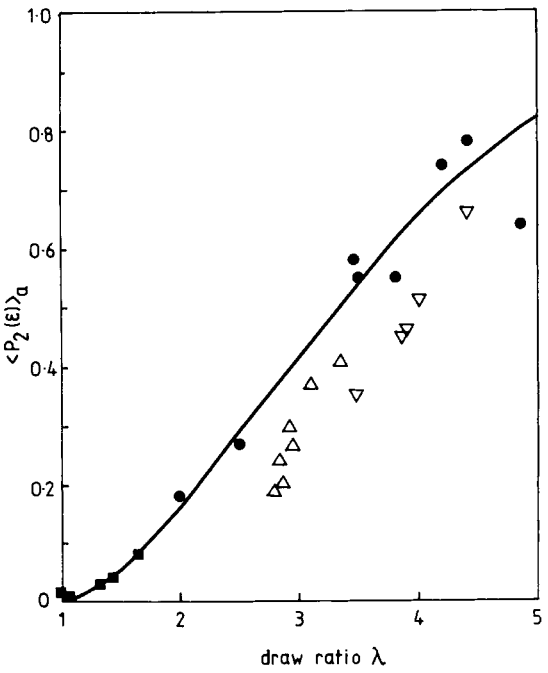

Fig. 2. $\langle P_2(\epsilon)\rangle_a$ plotted against draw ratio for samples in Tables I–IV. See Figure 1 for notation. Line is smooth curve through ●, ■.

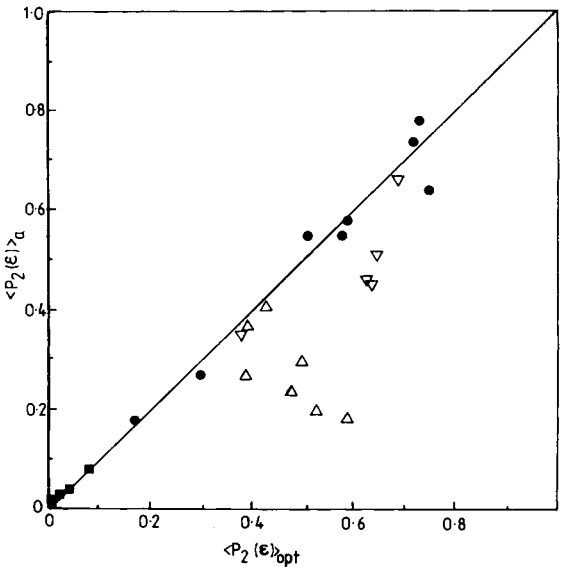

Fig. 3. $\langle P_2(\epsilon)\rangle_a$ plotted against $\langle P_2(\epsilon)\rangle_{opt}$ for samples in Tables I–IV. See Figure 1 for notation. Line is smooth curve through ●, ■.

drawn samples with $\lambda = 2$ appear to form a smooth sigmoidal curve (although the data do show more scatter at high draw ratios). The shrunk samples, however, consistently show lower values of $\langle P_2(\epsilon)\rangle_a$ than the drawn samples. When the crystalline drawn tapes are allowed to shrink, there is clearly a fall in amorphous orientation without a corresponding reduction in length. These results suggest that, whereas for shrunk samples originating from the sample with $\lambda = 2$ there are complementary and related falls in $\langle P_2(\epsilon)\rangle_{opt}$ and $\langle P_2(\epsilon)\rangle_a$, because both reflect the loss of overall orientation in a sample of negligible crystallinity, the shrunk samples prepared from higher draw ratio polymer show a fall in amorphous orientation but a smaller fall in overall orientation. This conclusion is brought out very clearly in Figure 3 which shows a comparison of $\langle P_2(\epsilon)\rangle_a$ with $\langle P_2(\epsilon)\rangle_{opt}$ for these samples. In this figure the straight line of unit slope shows the necessary relationship between $\langle P_2(\epsilon)\rangle_a$ and $\langle P_2(\epsilon)\rangle_{opt}$ for totally amorphous samples. The points for the drawn-only samples and those for the shrunk samples originating from the sample with $\lambda = 2$ necessarily lie close to this line because of the way in which $\langle P_2(\epsilon)\rangle_a$ was determined from $\langle P_2(\epsilon_M)\rangle$, using the method of Ref. 1. These samples are, however, of very low crystallinity and the values of $\langle P_2(\epsilon)\rangle_c$ are close to the values of $\langle P_2(\epsilon)\rangle_{opt}$, so that the true values of $\langle P_2(\epsilon)\rangle_a$ must be very close to those shown.

The Mechanical Behavior

In Figure 4 the Young's modulus values for all the samples are shown as a function of the final draw ratio. It can be seen that there is a reasonably smooth relationship between the modulus and the draw ratio for the drawn only samples and for samples drawn to $\lambda = 2.0$ and shrunk to different extents. For the latter samples, our previous work[2] suggests that there is negligible crystallinity introduced at drawing. It is therefore reasonable to find that the modulus correlates with the final draw ratio for such samples.

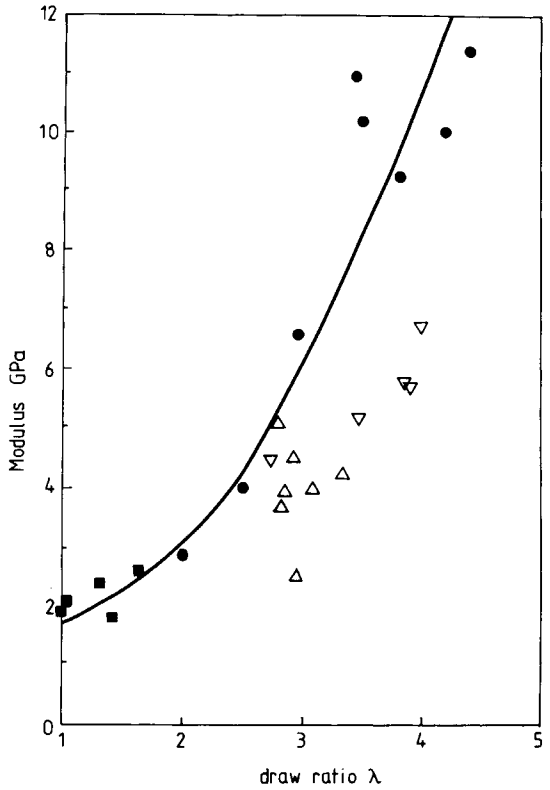

Fig. 4. Young's modulus plotted against draw ratio for samples in Tables I–IV. See Figure 1 for notation. Line is smooth curve through ●, ■.

The results are clearly very different for samples of higher initial draw ratio. The samples shrunk from $\lambda = 3.44$ (Table III) lie substantially below the line for drawn only samples. The same is true for another set of shrunk samples with initial draw ratios in the range 2.96–4.4 (Table IV). It can be concluded that where crystallisation occurs on drawing there is generally an appreciable fall in modulus on thermal treatment without a corresponding reduction in length. The situation is explored further by examining the modulus as a function of either $\langle P_2(\epsilon)\rangle_{\text{opt}}$ or $\langle P_2(\epsilon)\rangle_a$, which is shown in Figures 5 and 6, respectively. Although there is a moderately good correlation between the modulus and $\langle P_2(\epsilon)\rangle_{\text{opt}}$ for the drawn only samples and those shrunk from $\lambda = 2$, the other shrunk samples show much lower modulus values for a given value of $\langle P_2(\epsilon)\rangle_{\text{opt}}$. Recalling that $\langle P_2(\epsilon)\rangle_{\text{opt}}$ includes contributions from both the crystalline and amorphous regions, this result hints at the importance of the amorphous orientation. This is confirmed by inspection of Figure 6, which shows the modulus as a function of $\langle P_2(\epsilon)\rangle_a$. There is a better correlation, but substantial discrepancies for samples shrunk from $\lambda = 3.44$ to very low degrees of amorphous orientation. It is suggested that the explanation of these results is as follows: For low shrinkage temperatures and comparatively low shrinkages (Samples 15–17 in Table III and all samples in Table IV) the modulus falls due to the decrease in amorphous orientation. There is some increase in crystallinity, but this is comparatively small (from 0.06 to 0.22). The fall in modulus is very large (from 10.9 to 2.5 GPa).

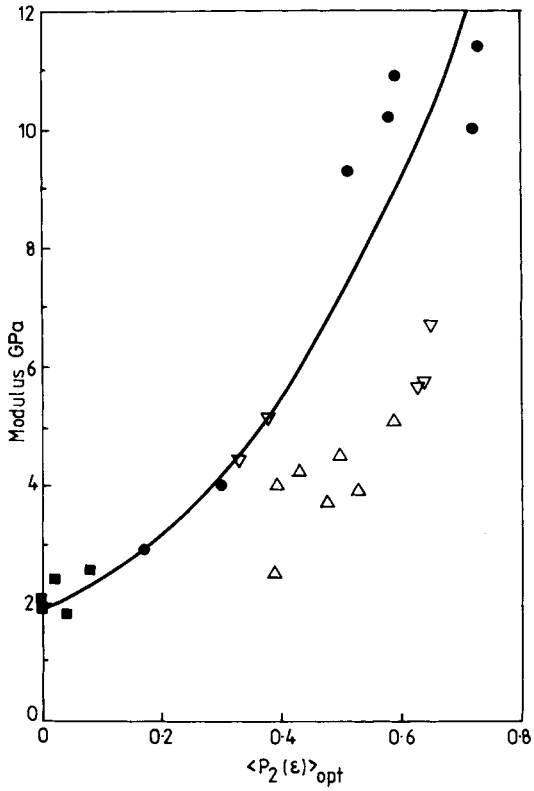

Fig. 5. Young's modulus plotted against $\langle P_2(\epsilon)\rangle_{opt}$ for samples in Tables I–IV. See Figure 1 for notation. Line is smooth curve through ●, ■.

In terms of a molecular interpretation, recalling the correlation of $\langle P_2(\epsilon)\rangle_a$ with $\langle P_2(\epsilon)\rangle_{trans}$ for drawn tapes,[3] the orientation of the trans conformers may be significant, and the thermal treatment may well be associated with a reduction in the orientation of trans conformations in the amorphous regions.

For samples shrunk at higher temperatures to higher degrees of shrinkage (samples 18–21 in Table III) there is a much smaller decrease in modulus (to between 2.52 and 5.09 GPa). At the same time the crystallinity increases from 0.22 to 0.49. The crystalline orientation is approximately constant, in the range 0.73–0.76, and there is a small decrease in amorphous orientation, (from 0.27 to 0.19). In the range where from sample to sample the modulus is *increasing* and the crystallinity is increasing at constant crystalline orientation, it has proved instructive to examine the predictions of simple Takayanagi models. Inspection showed that a simple parallel model was not consistent with the data, but a simple series model proved more applicable. This gives the modulus of the sample, E, as

$$\frac{1}{E} = \frac{f_c}{E_c} + \frac{1-f_c}{E_a} = (1-f_c)\left(\frac{1}{E_a} - \frac{1}{E_c}\right) + \frac{1}{E_c} \tag{2}$$

In Figure 7 the results for all samples in Table III are plotted in terms of $1/E$ against $(1-f_c)$. Also shown are two lines which can be regarded as representing bounds for theoretical predictions based on eq. (2). The amorphous material

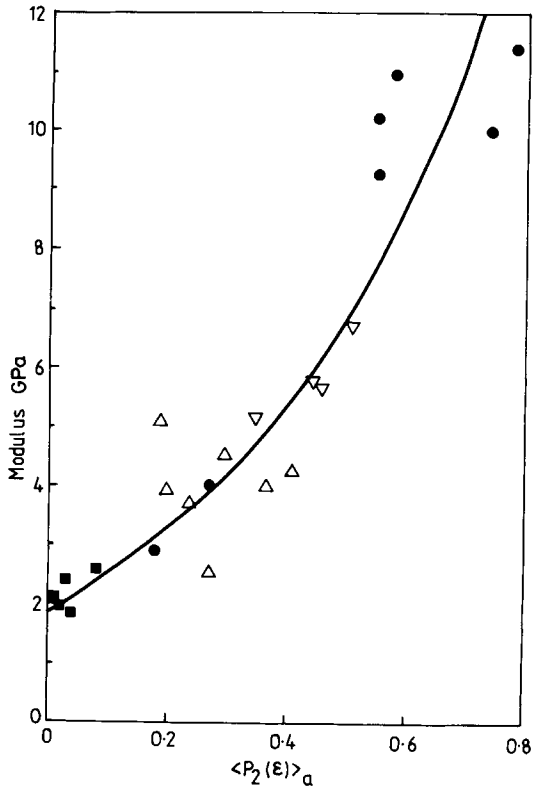

Fig. 6. Young's modulus plotted against $\langle P_2(\epsilon)\rangle_a$ for samples in Tables I–IV. See Figure 1 for notation. Line is smooth curve through ●, ■.

in all the samples of Table III, even after annealing, still shows appreciable orientation. The limiting value for $\langle P_2(\epsilon)\rangle_a$ is about 0.19, which corresponds to E_a = 3.1 GPa according to the curve in Figure 6. The crystal modulus for PET has been measured to be in the range 80–140 GPa,[5–7] so a value of E_c = 100 GPa has been chosen. These values for E_a and E_c give the dotted line shown in Figure 7. The crystalline material is not, however, fully oriented in these samples, for which the highest value of $\langle P_2(\epsilon)\rangle_c$ is 0.83. A value for E_c = 15 GPa, close to the highest modulus observed for unannealed PET fibers, was therefore taken as a lower bound, and this produced the full line in Figure 7.

The points for all samples except 17 and 4 lie fairly close to the predicted lines. The modulus for sample 17 is clearly anomalous, while the point for sample 4 would be expected to lie considerably below the lines because of the much higher degree of amorphous orientation for this sample compared with all others in Table III. The remaining points approach the line more closely as the region of constant crystalline and amorphous orientation is approached. Considering the simplistic nature of these calculations, it appears that the results are consistent with the view that the modulus is primarily related to the crystalline content and hence *increases* with shrinkage temperature and shrinkage due to the increase in crystallinity in a region where the crystalline and amorphous orientation are essentially constant.

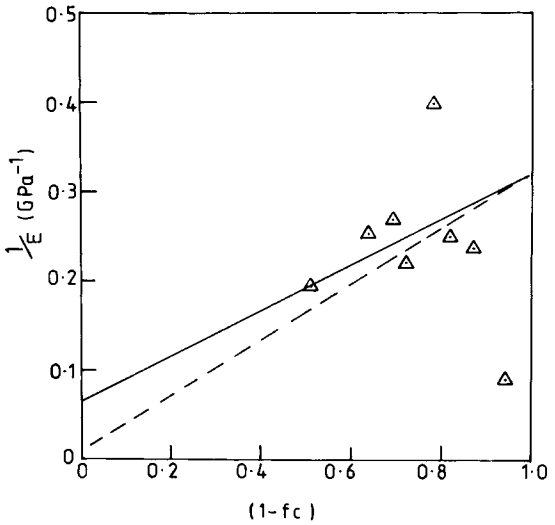

Fig. 7. Reciprocal of Young's modulus plotted against $1 - f_c$ for samples in Table III. See text for explanation of straight lines.

CONCLUSIONS

The mechanical results presented in this paper are consistent with the conclusions presented in our previous publication[3] on the effects of thermal treatment of drawn PET tapes. At low shrinkage temperatures the major effect is the disorientation of the amorphous regions. This leads to a decrease in the fluorescence orientation average without much increase in crystallinity, and there is a large fall in the modulus. At a molecular level this could well be associated with disorientation of the trans conformations in the amorphous regions. This interpretation would be consistent with the Prevorsek model for PET yarns,[8] where these highly oriented trans conformations in the amorphous regions are primarily responsible for the stiffness in a manner reminiscent of the Peterlin taut tie molecules. At higher shrinkage temperatures, there are small further falls in $\langle P_2(\epsilon)\rangle_a$; but the crystallinity increases substantially, and there is further shrinkage, which could be attributed to chain-folded crystallization. For these samples the changes in modulus can be modelled to a good first approximation by a simple series Takayanagi model.

It is therefore concluded:

(1) The low temperature shrinkage is due to disorientation of the amorphous regions, and this is reflected in the fall in $\langle P_2(\epsilon)\rangle_a$ determined by fluorescence. There is a large fall in Young's modulus and some crystallization. Shrinkage at higher temperatures is associated with a further smaller fall in amorphous orientation, but the crystallinity increases and there are corresponding *increases* in modulus.

(2) The Young's modulus of drawn PET tapes, and tapes shrunk from material with $\lambda = 2$ where there is no substantial crystallization, correlates with the overall molecular orientation. This is consistent with several previous investigations,[9] where the correlation between modulus and birefringence has been emphasized and the modulus/draw ratio relationship fitted on the basis of the aggregate

model,[10] which takes into account only changes in molecular orientation on drawing.

This research was undertaken as part of a research project financed by the Science and Engineering Research Council, and K.K.P.K-D also held an S.E.R.C. CASE studentship sponsored by I.C.I. Ltd., Fibres Division. We wish to thank Dr. C. G. Cannon for helpful discussions.

References

1. J. H. Nobbs, D. I. Bower, I. M. Ward, and D. Patterson, *Polymer*, **15,** 287 (1974).
2. J. H. Nobbs, D. I. Bower, and I. M. Ward, *Polymer*, **17,** 25 (1976).
3. J. H. Nobbs, D. I. Bower, and I. M. Ward, *J. Polym. Sci., Polym. Phys. Ed.*, **17,** 259 (1979).
4. V. B. Gupta and I. M. Ward, *J. Macromol. Sci. Phys.*, **B1**(1), 373 (1967).
5. W. J. Dulmage and L. E. Contois, *J. Polym. Sci.*, **28,** 275 (1958).
6. I. Sakurada, T. Ito, and K. Nakamae, *Bull. Inst. Chem. Res. Kyoto Univ.*, **42,** 77 (1964).
7. I. Sakurada and K. Kaji, *J. Polym. Sci.* **C31,** 57 (1970).
8. D. C. Prevorsek, P. J. Harget, R. K. Sharma, and A. C. Reimschuessel, *J. Macromol. Sci. Phys.*, **B8,** 127 (1973).
9. S. W. Allison and I. M. Ward, *Br. J. Appl. Phys.*, **18,** 1151 (1967).
10. I. M. Ward, *Proc. Phys. Soc.*, **80,** 1176 (1962).

Received September 17, 1982
Accepted October 8, 1982